

Modeling Airtanker Flight Distance between Concurrent Fires: The Development and Use of Statistical Distribution Parameters

Francis E. Greulich

Abstract: Airtankers, while actively engaging in initial attack, are sometimes reassigned and flown directly to another randomly occurring initial attack fire. Airtanker system planning that means to incorporate this fire-to-fire transfer activity needs information about the flight distance between these randomly located fires. Moments of the distance distribution, derived in this article, can be used to characterize and evaluate fire-to-fire airtanker dispatch within and between protection areas. A hypothetical example illustrates how a proposed change in an airtanker protection zone can affect not only airbase-to-fire flight distance but also fire-to-fire flight distance. In this example, the expected airbase-to-fire distance and the expected total transfer-flight distance are both significantly reduced, but at the same time, somewhat unexpectedly, the average fire-to-fire flight distance actually increases. The discovery and quantification of such unanticipated results can potentially influence airtanker system design. These key system design parameters can now be obtained through the exceedingly fast and accurate analytical methods presented here. *FOR. SCI.* 54(1):47–57.

Keywords: operations research, transportation planning, expected distance, polygonal regions

AS RECOUNTED IN A PREVIOUS ARTICLE (Greulich 2003), the managerial utility of wildland fire resource allocation models depends fundamentally on the accurate description and estimation of travel distances to initial attack fires. That article and a subsequent one (Greulich 2005) showed how two airtanker flight distance parameters, the expected flight distance and the variance of flight distance, can be determined with incomparable speed and accuracy using closed form equations. This third article addresses the determination of these flight distance parameters for randomly located points within polygonal regions and thus concludes the analytical development of closed form equations for these flight distance parameters.

Some previous research has been done on the calculation of random distance parameters within and between polygonal regions. An overview of this research begins the presentation. After this review, an example, taken from the first article of the series and extended, provides an introduction to the specific airtanker transfer topic of interest. Provided with a motivational problem description, the reader who is interested in the analytical development may, at this point in the presentation, consult the detailed development of a general solution in the appendixes. The main body of the article continues with verification of the analytical solution and its software implementation. The presentation then moves to an analytical solution and interpretation of the illustrative airtanker transfer problem. Some thoughts on possible future research directions conclude the article.

Previous Research

The role of airtankers in initial attack and the work of analysts in the modeling of this fire control activity have previously been discussed (Greulich 2003). The issue of

fire-to-fire transfer of airtankers has not been the subject of much prior research, and readers are referred to Greulich (2005) for a discussion of the limited work published on this aspect of airtanker modeling.

Some research results on the statistical description of the distance between randomly located points within and between planar regions have been previously reported in the literature. In 1877 Professor Morgan Crofton presented a general formula for the mean value of the distance between two points taken at random within a convex area. Much later, Santaló (1979) used this result to obtain the expected distance between two random points within a circle, an equilateral triangle, and a rectangle. It was Ghosh (1943a), however, who appears to have given the first explicit formulation of the mean and variance equations for random distances within any rectangle. Before Ghosh, Borel (1925) had presented derivations of the distribution function for the random distance within a circle, a triangle, and a square. His derivation for the circle is correct, as confirmed by Kendall and Moran (1963). However, his derived distribution function for the square is seen to be incomplete compared with the density function correctly derived and used for the calculation of moments by Ghosh. Similarly incomplete is Borel's derivation for the distribution function of a general triangle. That deficiency in the derivation also nullifies his proposed evaluation procedure for random distances within a general, convex polygonal region. Borel's fundamental error is a failure to account for discontinuities that occur within the range of the random distance variable. This characteristic of triangular and rectangular figures, in contrast to the distance continuity provided by a circle, is essential to the complete and, therefore, correct derivation. Ghosh recognized and appropriately incorporated this discontinuity into his derivations. Ruben (1978), motivated by

Francis E. Greulich, College of Forest Resources, University of Washington, Seattle, WA 98195-2100—Phone: (206) 543-1464; Fax: (206) 685-3091; greulich@u.washington.edu.

Manuscript received July 18, 2006, accepted July 6, 2007

Copyright © 2008 by the Society of American Foresters

the many practical applications for the moments of random distances between polygons, presented a lengthy procedure for their calculation. Unfortunately, his procedure is not easily applied, and what testing has been reported raises doubts about its results. Vaughan (1984), a renowned researcher in transportation science, wrote that Ruben's formulas "are far too cumbersome for practical use" and later determined that the formulas give "poor results in certain common configurations" (Vaughan 1987). A more recent publication is that of Okabe and Miller (1996), who give a formula and computational procedure to calculate the average distance between two polygons. They apply their formula and procedure to square elements in a variety of configurations. Their results and those of other researchers are reported and compared during the verification process described in this article.

An Illustrative Example

In a previous article (Greulich 2003) a hypothetical airtanker initial attack (ATIA) zone was described. That protection zone is reproduced here in Figure 1 [1]. An airbase, indicated with a starburst in Figure 1, is located at coordinate location (400,400); these coordinates are given in kilometers east and north of the coordinate system origin. For this location the expected one-way flight distance from the airbase to an initial attack fire was, in the previous article, determined to be 196 km, and the SD was determined to be 77.4 km. These are exact population parameter values, to the given number of significant digits, for the statistical distribution of random flight distances under the assumed fire-start conditions; viz., the polygonal partition within which a fire starts is randomly determined according to the specified partition probability and, given the partition, the precise point of fire start is determined by a continuous uniform probability distribution defined across the area of

the selected partition. For purposes of this development, all initial attack fire starts across the protection region are assumed to be independently distributed [2].

In the second article of this series (Greulich 2005), it was reported from the literature that there are circumstances under which airtankers may be transferred between two initial attack fires. For purposes of modeling airtanker system performance with greater accuracy it is desirable to numerically describe the randomly occurring transfer distance between initial attack fires. This information can be of special interest when one is evaluating different airtanker types, initial attack boundaries, or airtanker dispatch rules. An accurate numerical characterization of the fire-to-fire flight distance is anticipated to be of even greater relevance if these transfers tend to occur during periods of extreme fire conditions and concomitant congestion of the initial attack system (Islam and Martell 1998). It is during these "fire flaps" that airtanker allocation decisions are most likely to have major consequences in fire control efforts.

In this second article a procedure was given for calculating the flight distance parameters for fire starts on portions of the initial attack protection area that can be most effectively described by line segments. Of even greater interest and modeling utility, however, is the statistical characterization of the random flight distance between fire-start locations within and between portions of the protection zone that are best described by polygonal regions. The protection zone shown in Figure 1 provides an illustrative, hypothetical example of this modeling situation.

In fire-control planning scenarios, airbase zones of initial attack jurisdiction may be redefined during plan development and evaluation. As initial attack boundaries are redrawn, the expected performance of airtankers stationed at the airbase changes. Changes in protection area boundaries almost certainly lead to changes in dispatch distances and with these changes in airtanker flight distance come attendant changes in system performance. One simple hypothetical planning scenario might involve the reassignment of initial attack responsibility for the partitioned area labeled D in Figure 1 to an adjacent airbase. To better understand the impact of such a reallocation of initial attack jurisdiction, its impact on airbase-to-fire dispatch distances should be considered. Likewise, the impact of changes in fire-to-fire flight distance should also be considered, if that dispatch practice is likely to occur. The proposed analytical procedure of this article, when applied to this example, can illustrate its potential role in such planning.

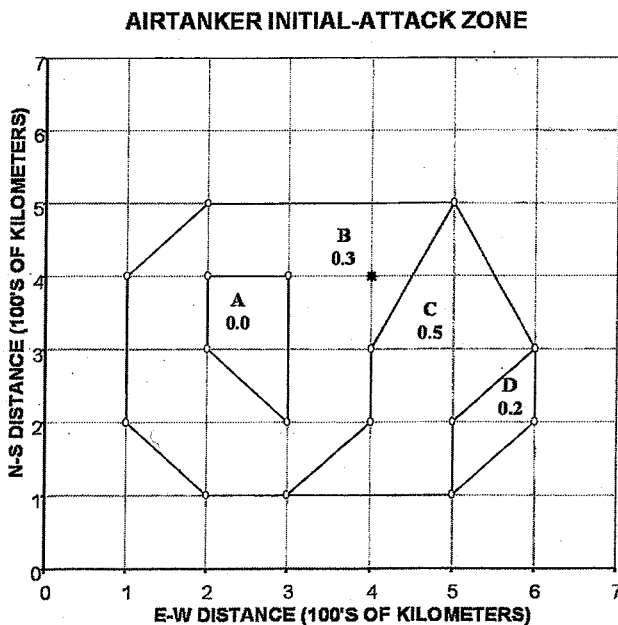


Figure 1. Hypothetical ATIA protection zone defined by four polygonal regions, one of which, A, is a protection-excluded enclave.

The Analytical Procedure

An analytical procedure has been developed and software written to calculate the first two population moments about the origin for the random distance between any two polygonal regions in the plane [3]. The two polygonal regions may be spatially separated or overlapping in all or part. The individual regions themselves can be disjoint and (or) have excluded enclaves; in short, there are no convexity limitations on the individual polygonal regions.

The derivation of the analytical results follows the same general approach used in the preceding article (Greulich

2005). This development is detailed in Appendix A, in which the first two moments are derived for the length of a line segment between two points. Each point is randomly located within a trapezoidal area. All trapezoids are uniquely oriented for this analysis; they have two opposite sides that parallel the y -axis and a base formed by the x -axis. No other restrictions apply; e.g., the trapezoids may overlap or be spatially separated. For convenience and clarity of exposition they are shown in the first quadrant of the coordinate system, but that is not required.

These analytical results for trapezoids are readily extended to general polygonal regions using the familiar coordinate area formula. The use of the coordinate area formula in this particular application is described in Appendix B. The fundamental computational requirement of the procedure is made clear at this point. All combinations of sides for the two polygonal regions must be evaluated; i.e., if one region has m sides and the other n , then mn combinations must be evaluated. This computational requirement for the general region-to-region problem has been identified previously by Okabe and Miller (1996).

Verification of the Procedure

Verification of the proposed analytical procedure is based on a comparison with previously published results and procedures given by other authors and by the results of an independently developed numerical analysis model. The analytical and numerical results reported by Ghosh (1943a, 1943b, 1951) have been independently derived and calculated many times (Oser 1976, Conolly 1981, Gaboune et al. 1993). The only results found in the literature that conflict with those given by Ghosh and by the other researchers cited here are those presented in Okabe and Miller (1996), who seemed to be unaware of previous research on this specific topic. Given overwhelming confirmation of Ghosh's results, they are presented in Table 1 for a side-by-side comparison with results from the analytical model proposed in this article.

Results from the analytic model for more complex transfer region configurations were verified using the numerical integration model described in Appendix C. Various inter- and intra-area transfer configurations were formed and analyzed using the coordinate points mapped in Figure 2. Table 2 gives the results obtained from the program when it was applied to the indicated configurations. Numerical integration for confirmation of the results beyond three decimal places generally proved to be too time-consuming. For

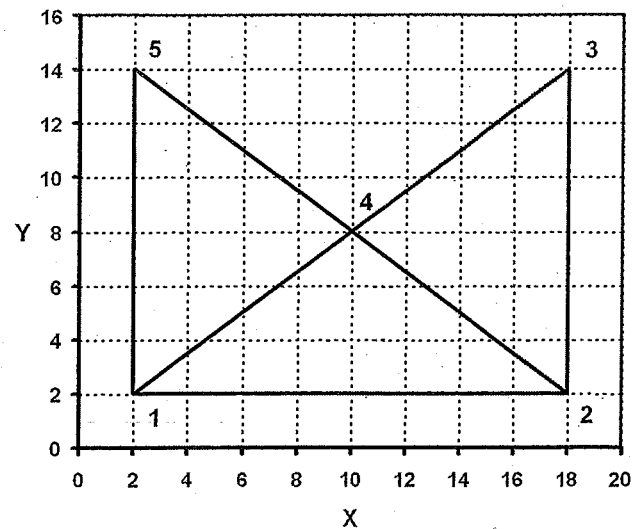


Figure 2. Plotted regions for analyzing alternative region-to-region configurations for random distance moment calculations.

example, to verify the mean value to three decimal places by numerical integration for the first entry of Table 2, it took a Fortran program approximately 55 seconds on a Pentium 4 (2.53 GHz) computer. With the procedure of this article used in a Fortran program the exact answer was calculated in approximately 0.055 second on the same computer. This comparative result, however, limited as it is, shows a 3 order-of-magnitude difference in the time requirements for this particular computation. All values shown in this article have been confirmed by numerical integration to the number of significant figures shown, with rounding of the last digit.

Results given by the analytical model are invariant with respect to coordinate system placement. The same results given in Table 2 may be obtained using the coordinates listed in Table 3. These are new coordinates for Figure 2 after translation and rotation. The origin of the coordinate system is now interior to the figure which has vertices in all four quadrants. This computational invariance is an important practical aspect of the analytical procedure.

Illustrative Example Continued

As mentioned, one possible reconfiguration of the original ATIA protection zone might involve removing area D from the protection zone of the airbase (Figure 1). An immediate question of interest to planners might be the

Table 1. Comparison of the results reported by Ghosh with those calculated using the proposed analytical procedure of this article

Configuration	Mean, taken from Ghosh (1951)	Mean, calculated by the author	Variance, taken from Ghosh (1943a)	Variance, calculated by the author
1 × 1 square	0.521	0.521	0.061	0.061
1 × 2 rectangle	0.804	0.805	0.084 ^a	0.186
2 adjacent 1 × 1 squares	1.088	1.088	NA	0.149
2 diagonal 1 × 1 squares ^b	1.473	1.474	NA	0.162

^aThis is a misprint in Ghosh (1943a); the corrected value using Ghosh's equations is 0.186. Other minor differences are due to rounding of the current author's analytically calculated values to three decimal places.

^bThe two squares touch at a common vertex on a shared diagonal.

Table 2. Means and standard deviations calculated for different polygon configurations

Transfer configuration as taken from Figure 2	Comment	Mean μ	SD σ
123451 ↔ 123451	Transfer within a single nonconvex region	7.185	3.821
1231 ↔ 1241	Transfer between two regions, one of which is completely overlapped by the other	5.948	3.260
1451 ↔ 2342	Transfer between two spatially separated regions	11.176	2.825
1231 ↔ 1451	Transfer between adjoining regions	9.361	3.486
1231 ↔ 1251	Transfer between partially overlapping regions	7.654	3.782

Table 3. Coordinates for the vertices of the nonconvex region 123451 of Figure 2 when located arbitrarily on a Cartesian coordinate system

Point i	Coordinate Pair	
	X_i	Y_i
1	-4.0000	-13.1716
2	7.3137	-1.8579
3	-1.1716	6.6274
4	2.5858	-3.2721
5	-12.4853	-4.6863
6 = 1	-4.0000	-13.1716

potential impact of this reconfiguration on ATIA system response time. Some insight into the potential impact of this protection zone modification can be provided by a good estimate of the change in initial attack airbase-to-fire travel distance (and therefore flight time). Procedures described in

the first article of this series show that removal of area D shortens the expected flight distance from the given airbase location to an initial attack fire from 196 to 182 km, a reduction of 7% in the expected flight distance. It is also found, using these previously presented procedures, that there is only minimal impact on variability in airbase-to-fire flight distance. The SD of flight distance drops slightly, from 79 to 77 km. The relative consistency in flight distance to fires from the airbase should continue at the same level under the proposed reconfiguration.

A second consideration is the impact of the reconfiguration on a fire-to-fire reallocation dispatch. Using the analytical methodology and computational procedures of this article the expected fire-to-fire flight distance results shown in Table 4 have been obtained. On most sorties the airtanker attacks a single fire and returns to its airbase; transfer to a

Table 4. Fire-to-fire flight distance parameters calculated for the original and reconfigured initial attack protection zone

		Original protection zone			Reconfigured protection zone		
		Ab/B/B/Ab	Ab/C/B/Ab	Ab/D/B/Ab	Ab/B/B/Ab	Ab/C/B/Ab	NA
All permissible flight patterns ^a		Ab/B/C/Ab	Ab/C/C/Ab	Ab/D/C/Ab	Ab/B/C/Ab	Ab/C/C/Ab	NA
		Ab/B/D/Ab	Ab/C/D/Ab	Ab/D/D/Ab	NA	NA	NA
		Ab/B/Ab	Ab/C/Ab	Ab/D/Ab	Ab/B/Ab	Ab/C/Ab	NA
P{X} ^b	B	X	D	B	X	D	
	0.3	C	0.2	0.375	C	NA	
P{Y X} ^c	B	C	D	B	C	D	
	Y	0.120	0.040	0.020	0.120	0.040	
	C	0.040	0.080	0.050	0.040	0.080	
	D	0.010	0.020	0.050	NA	NA	
P{Pattern} ^d	Ab	0.830	0.860	0.880	0.840	0.880	
		0.036	0.020	0.004	0.045	0.025	
		0.012	0.040	0.010	0.015	0.050	
		0.003	0.010	0.010	NA	NA	
E{Dist; X→Y} ^e	B	C	D	B	C	D	
	Y	191.1	260.2	329.2	191.1	260.2	
	C	260.2	139.8	150.7	260.2	139.8	
	D	329.2	150.7	61.2	NA	NA	
E{Dist Pattern} ^f	Ab	190.6	176.3	253.9	190.6	176.3	
		572.2	627.1	773.6	572.2	627.1	
		627.1	492.4	580.8	627.1	492.4	
		773.6	580.8	568.9	NA	NA	
E{Dist}	381.1	352.6	507.7	381.1	352.6	NA	
	418.9			389.4			

^a Each permissible flight pattern starts and ends at the airbase (Ab). Only one fire-to-fire transfer is a possibility before returning to the airbase.

^b Given that an ATIA fire has occurred in the protection zone of the airbase, the probability that it is in area X.

^c Probability of sending the AT currently assigned to an ATIA fire in area X directly to a second ATIA fire in area Y or, alternatively, back to the airbase.

^d Probability of each of the listed permissible flight patterns; i.e., P{Y|X} P{X}.

^e Expected one-way flight distance from a fire in area X to a fire in area Y (calculated using the analytical procedure of this article) or the distance between X and the airbase (based on the procedures and results found in Greulich 2003).

^f Expected total flight distance including distance from the airbase to the first ATIA fire, distance from the first fire to the second, if a second fire occurs, and the return distance to the airbase; listed values correspond to the specified flight patterns.

second fire would be the exception. This likely operational characteristic has been acknowledged through the assigned conditional transfer probabilities, $P\{Y|X\}$. It should be noted that these reallocation probabilities would, in practice, be empirical probabilities based on observed ATIA fire occurrence under specific fire-related conditions during a specified period of time. It is convenient for the illustrative purposes of this article to assume that these ATIA fire occurrence and airtanker reallocation probabilities are for any day during the fire season that meets specific ATIA fire-related conditions. Such conditions may include, for example, the fire danger rating classification for an area [4]. The conditional reallocation probabilities of Table 4 may also reflect past, or planned, fire-to-fire dispatch policy as well as empirical probabilities based on historically observed overlapping ATIA fires.

All of the flight patterns to be analyzed in this example are shown at the top of Table 4. The probability of observing each possible pattern and its expected total transfer-flight distance for this day-type have been calculated and are listed in the table. The sum product of these probabilities and their associated transfer-flight distances yield the expected total transfer-flight distance parameter for the protection zone on this day-type. The expected sortie transfer-flight distance for the original and reconfigured zone are 419 and 389 km, respectively [5]. These values represent a 7% decrease in the expected transfer-flight distance for ATIA fires occurring on this day-type with these sortie patterns and probabilities. In restricting attention only to fire-to-fire flight distances and ignoring the flight segments out of and returning to the airbase, the expected flight distance during reallocation transfer goes from 184 to 193 km. This is an unanticipated 4% increase in flight distance during reallocation under the new configuration.

In summary then, the proposed change in protection zone configuration might be expected to reduce the distance flown from the airbase to an initial attack fire from 196 to 182 km; however, the distance to be flown to a second fire, when it occurs concurrently with the first and direct transfer reallocation takes place, actually increases from 184 to 193 km. This increased fire-to-fire flight distance would have been hard to anticipate in the absence of this analytical assessment.

Continuing with the impact analysis, it is noted that the expected number of initial attack fires falling under the jurisdiction of the airbase on this day-type will drop by 20% under this new protection zone configuration. If initial attack jurisdiction for these fires is reassigned to another airbase, the impact assessment on total airtanker system performance should include an examination of the second airbase's fleet and infrastructure response. Such system level changes must be considered in assessing the ultimate cost-effectiveness of the reconfiguration.

Concluding Observations

These analytical results and their software implementation represent a different way of specifying, through the use of statistical distribution parameters, the travel distances associated with random fire-start occurrence. Exceptional

accuracy and low computation times may now make it feasible to modify existing models to more effectively accommodate operational fire-to-fire transfer activity. These results place the specification of key travel distance parameters on a firm analytical footing, a foundation that has been verified using results taken from a wide range of independent sources and alternative methods of derivation. A completely general, polygon-to-polygon, statistical parameter description of straight-line travel distance between random points is now available to researchers.

New modeling opportunities are opened up by the analytical approach presented in this and the preceding two articles. The spatial occurrence of fire starts is quite descriptively and flexibly based on the geometric elements of points, line segments, and polygonal regions. The rapid and accurate summary specification of travel distance to random fire occurrence locations within a protection zone, the boundaries of which can be redefined on the fly, has the potential to open up new modeling applications for which computational time has been a restricting factor.

At a more basic level, knowledge of the population mean and variance gives rise to the possibility of applying probabilistic inequalities (Savage 1961) to a range of management problems. In the case of probabilistic inequalities the development of other moments of the distribution by the methodology shown in the three articles of this series can widen the choice and sharpen the bounds of these probabilistic inequalities. When working with the mean of multiple fire starts, it is anticipated that the analyst will now be able to appeal to the central-limit theorem even under the expectation of relatively few fire-start occurrences within the period and (or) area of interest. It is possible that many fire-start distance distributions will have a shape that requires only a few observations to achieve an approximation that is adequate for most operational uses [6]. Probabilistic manipulation of these new parameters makes the application of more advanced techniques, such as chance-constrained programming and queuing system bounding and approximation methods, potential decision tools for airtanker management.

There remain research questions, the solutions to which would enhance the applicability of this approach to modeling airtanker system behavior. For example, the assumption of statistical independence in fire starts merits careful examination. There may be applications in which modeling under the assumption of statistical independence will give unacceptably poor or misleading results, e.g., the recurrent observation of lightning and arson fires during periods of extreme fire weather. Research that incorporates advances in relevant topics such as space-time clustering should be a high priority under these conditions. Also, as previously mentioned, there may be a need to know the higher moments of the distance distribution. In this regard it would appear that the current derivational procedure may be suitable for their development as well.

Finally, it is hoped that the lengthy formulas and computational procedures of these three articles will soon be expressed in additional software implementations that are readily accessible to a wider range of users. At the present

time no commercial geographic information systems package can generate these parameters. Until easily used software routines are available it seems likely that these results will not be widely used outside the research community. It is with this expectation of future software development that the detailed formula descriptions and worked examples of these articles have been provided. It is hoped that this in-depth presentation of the material will facilitate the transition of these procedures from a research methodology to a commonly applied tool in wildfire control.

Endnotes

- [1] Reproduced in accordance with the Research Press Policy of the National Research Council (NRC) of Canada.
- [2] Fire starts are distributed as a homogeneous Poisson process within each partition.
- [3] An executable Fortran program for the calculation of the polygon-to-polygon travel parameters described in this paper may be downloaded from the following website: faculty.washington.edu/greulich/Research.htm
- [4] For an example of the identification and development of similar empirical probabilities the interested reader is referred to Greulich and O'Regan (1975).
- [5] Distances flown to water pickup points while fighting the fire are excluded from all calculations in this example.
- [6] Good judgment and empirical evidence may be required in estimating the number of fire starts needed to achieve a sufficiently close approximation to the normal distribution; see Snedecor and Cochran (1980) for two contrasting examples.

Literature Cited

- BOREL, E. 1925. Principes et formules classiques du calcul des probabilités: leçons professées à la Faculté des Sciences de Paris, par M. Émile Borel, rédigées par M. René Lagrange, in *Traité du calcul des probabilités et de ses applications*, t. I, fasc. I. Gauthier-Villars, Paris, France. 158 p.
- CONOLLY, B. 1981. *Techniques in operational research*, Vol. 2: *Models, search and randomization*. John Wiley & Sons, New York, NY. 340 p.
- CROFTON, M.W. 1877. Geometrical theorems relating to mean values. *Proc. London Math. Soc.* VIII:304–309, England.
- DAHLQUIST, G., AND A. BJÖRCK. 1974. *Numerical methods*. Prentice-Hall, Inc., Englewood Cliffs, NJ. 573 p.
- GABOUNE, B., G. LAPORTE, AND F. SOUMIS. 1993. Expected distances between two uniformly distributed random points in rectangles and rectangular parallelepipeds. *J. Opt. Res. Soc.* 44(5):513–519.
- GHOSH, B. 1943a. On the distribution of random distances in a rectangle. *Ind. Sci. News Assoc. Calcutta Sci. Cult.* 8(9):388.
- GHOSH, B. 1943b. On random distances between two rectangles. *Ind. Sci. News Assoc. Calcutta Sci. Cult.* 8(11):464.
- GHOSH, B. 1951. Random distances within a rectangle and between two rectangles. *Bull. Calcutta Math. Soc.* 43(1):17–24.
- GREULICH, F.E. 2003. Airtanker initial attack: A spreadsheet-based modeling procedure. *Can. J. For. Res.* 33(2):232–242.
- GREULICH, F.E. 2005. Airtanker flight distance between fires: Random fire starts on line segments. *For. Sci.* 51(5):460–471.
- GREULICH, F.E., AND W.G. O'REGAN. 1975. Allocation model for air tanker initial attack in firefighting. US For. Serv. Res. Note PSW-301. 8 p.
- ISLAM, K.M.S., AND D.L. MARTELL. 1998. Performance of initial attack airtanker systems with interacting bases and variable initial attack ranges. *Can. J. For. Res.* 28(10):1448–1455.
- KENDALL, M.G., AND P.A.P. MORAN. 1963. *Geometrical probability*. Hafner Publishing Company, New York, NY. 125 p.
- MORTENSON, M.E. 1995. *Geometric transformations*. Industrial Press, Inc., New York, NY. 400 p.
- OKABE, A., AND H.J. MILLER. 1996. Exact computational methods for calculating distances between objects in a cartographic database. *Cartog. Geog. Inform. Sys.* 23(4):180–195.
- OSER, H.J. 1976. Problem 75-12, an average distance. *SIAM Rev.* 18(3):497–500.
- RUBEN, H. 1978. On the distance between points in polygons, in *Lecture notes in biomathematics* 23, Miles, R., and J. Serra (eds.). Springer-Verlag, Berlin, Germany.
- SANTALÓ, L.A. 1979. *Integral geometry and geometric probability*. Addison-Wesley Publishing Co., Reading, MA. 404 p.
- SAVAGE, I.R. 1961. Probability inequalities of the Tchebycheff type. *Natl. Bur. Stand. J. Res. Sect. B Math. Math. Phys.* 65B(3):211–222.
- SHIH, T-Y. 1995. Area computation by coordinates. *J. Surv. Eng.* 121(4):145–154.
- SNEDECOR, G.W., AND W.G. COCHRAN. 1980. *Statistical methods*, 7th ed. Iowa State University Press. Ames, IA. 507 p.
- VAUGHAN, R.J. 1984. Approximate formulas for average distances associated with zones. *Transport. Sci.* 18(3):231–244.
- VAUGHAN, R.J. 1987. *urban spatial traffic patterns*. Pion Limited, London, England. 334 p.

Appendix A

The derivations of this appendix follow the pattern established in a previous article (Greulich 2005). First, a similarity transformation is applied to the geometric elements of interest (Mortenson 1995). Next, a statistical procedure developed by Crofton (Kendall and Moran 1963) is applied, and the resulting differential equation is solved for the desired result. The total derivation proceeds stepwise, with each step building on previous results. For example, to develop the expected distance from a line to a trapezoid, the previously derived expected distance from a point to a line (Greulich 2003) and the expected distance between line segments (Greulich 2005) must be used. The development of this article starts with the derivation of the first moment about the origin for the distance between one randomly located point on a line segment and a second randomly located point within a trapezoid.

Consider the trapezoid and separate line segment of Figure A1. By suitable translations any line-trapezoid combination of relevance to this development can be moved so that the line segment starts at the origin of the axes as illustrated. The general location of the trapezoid is irrelevant, but note that two of its sides are parallel to the y-axis. The selection of this orientation for the trapezoid is essential to follow-on developments.

A dilation transformation about the origin is now applied (Mortenson 1995). A dilation factor, k , can result in an expansion ($k > 1$) or contraction ($0 \leq k < 1$) of the plotted geometric elements. In this instance the dilation factor is set equal to $1 + \Delta K$, where $\Delta K > 0$. An arbitrary reference point, y , may be selected on the positive branch of the y-axis. On applying the dilation factor the value of y is changed to y' ; i.e., $y' = ky$. Defining $y' - y \equiv \Delta y$, it may then be shown that $\Delta K = \Delta y/y$. In a similar fashion, the length, L , of any line segment has been increased by an amount ΔL . The length, L' , of a dilated line may be calculated as $L' = (L + L\Delta K)$, and $\Delta L/L = \Delta K$. Likewise the coordinates of any arbitrary point (x_i, y_i) are, after dilation,

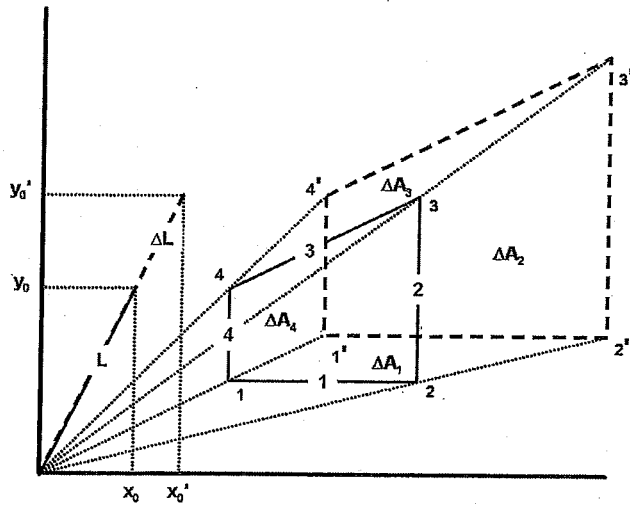


Figure A1. A dilation transformation about the origin (radiating dotted lines) is applied to a line segment and trapezoid (solid lines) giving the transformed line segment and trapezoid (dashed lines).

given by $(x_i', y_i') = (x_i + x_i\Delta K, y_i + y_i\Delta K)$. Again referring to Figure A1, note the convention followed here: corner indexing on the trapezoid will always start with the lower left corner and proceed in a counterclockwise fashion. Each side of the trapezoid is also numbered, starting with the lower boundary and moving counterclockwise. These side lengths of the trapezoid are labeled L_i . By virtue of the dilation, the area, A , of the original trapezoid has increased by an amount ΔA . These incremental areas are labeled in concert with their respective sides as ΔA_i . Inspection of the specific configuration in Figure A1 reveals that for small increments, ΔA_2 and ΔA_3 add to the total area, whereas ΔA_1 and ΔA_4 reduce the original area so that $A' = A - \Delta A_1 + \Delta A_2 + \Delta A_3 - \Delta A_4$. The respective counterclockwise listed corner indices for each of these incremental areas are $(122'1')$, $(22'3'3')$, $(433'4')$, and $(11'4'4')$. Recall that one form of the coordinate area formula may be written as

$$\text{Area} = \frac{1}{2} \sum_{i=1}^4 (x_i y_{i+1} - x_{i+1} y_i), \quad (\text{A1})$$

where $(x_5, y_5) \equiv (x_1, y_1)$, and a counterclockwise orientation is observed (Shih 1995). Applying this formula to the four incremental areas defined by their above-listed corner indices, the following approximations are obtained after ΔK^2 terms have been dropped and $\Delta K = \Delta y/y$ is inserted:

$$\Delta A_1 \approx (x_2 y_1 - x_1 y_2) \left(\frac{\Delta y}{y} \right), \quad (\text{A2a})$$

$$\Delta A_2 \approx (x_2 y_3 - x_3 y_2) \left(\frac{\Delta y}{y} \right), \quad (\text{A2b})$$

$$\Delta A_3 \approx (x_3 y_4 - x_4 y_3) \left(\frac{\Delta y}{y} \right), \quad (\text{A2c})$$

and

$$\Delta A_4 \approx (x_1 y_4 - x_4 y_1) \left(\frac{\Delta y}{y} \right). \quad (\text{A2d})$$

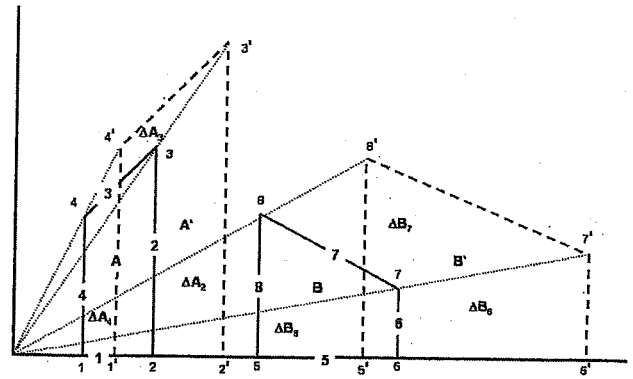


Figure A2. A dilation transformation about the origin (radiating dotted lines) is applied to two trapezoids (solid lines) giving the transformed trapezoids (dashed lines).

Crofton's procedure is now applied. One point will be located, at random, along the length $L + \Delta L$, and a second point will be randomly located on the area $A + \Delta A$. By conditioning on all possible locations of the two randomly located points, the expected distance, G , from one of these points to the other can be written as

$$G(y + \Delta y) = \left[\frac{1}{(A + \Delta A)(L + \Delta L)} \right] \times [ALG(y) - \Delta A_1 L F_1 + \Delta A_2 L F_2 + \Delta A_3 L F_3 - \Delta A_4 L F_4 + \Delta L E\{D_A\}]. \quad (\text{A3})$$

$G(y + \Delta y)$ is the mean distance after the dilation, and $G(y)$ is the mean distance before the dilation. F_i is the expected distance from line segment L to the line approached in the limit as the area ΔA_i becomes infinitesimally small; i.e., ΔK goes to 0. The value of F_i is found via formulas given in a previous publication (Greulich 2005). The actual procedure used to calculate each F_i depends on whether the line segment L is parallel, or not, to trapezoid side L_i . It is also to be noted that if line segment 2 or line segment 4 has zero length, the respective ΔA_i contribution is also 0. The formula for the expected distance, $E\{D_A\}$, is also found in a previous publication (Greulich 2003). In this case the expectation is that for the random distance from the end point of line segment L to a random point within the trapezoid area A . Note here also that evaluation of the expected distance is based on the limiting location, the end of line segment L as ΔL goes to 0 and the limiting (original) area A as ΔA goes to 0.

Inspecting the specific case illustrated in Figure A1 from which formulas A2a–A2d were written it is possible to write

$$\Delta A = -\Delta A_1 + \Delta A_2 + \Delta A_3 - \Delta A_4. \quad (\text{A4})$$

Now, after substituting for the incremental areas on the right using Equations A2a–A2d and reducing, it is found that

$$\Delta A \approx 2A \left[\frac{\Delta y}{y} \right]. \quad (\text{A5})$$

Substitute A5 into the denominator of Equation A3 to

obtain, after eliminating the $(\Delta y/y)^2$ term,

$$G(y + \Delta y) = \left[\frac{1}{AL + 3AL(\Delta y/y)} \right] \times [ALG(y) - \Delta A_1 LF_1 + \Delta A_2 LF_2 + \Delta A_3 LF_3 - \Delta A_4 LF_4 + A\Delta LE\{D_A\}]. \quad (A6)$$

Subtract $G(y)$ from each side, divide each side by Δy , substitute for A_i using Equations A2a–A2d, and cancel terms to obtain

$$\frac{G(y + \Delta y) - G(y)}{\Delta y} = \left[\frac{1}{A + 3A(\Delta y/y)} \right] \times \left[\left(\frac{-3A}{y} \right) G(y) - \left(\frac{x_2 y_1 - x_1 y_2}{y} \right) F_1 + \left(\frac{x_2 y_3 - x_3 y_2}{y} \right) F_2 + \left(\frac{x_3 y_4 - x_4 y_3}{y} \right) F_3 - \left(\frac{x_1 y_4 - x_4 y_1}{y} \right) F_4 + \left(\frac{A}{y} \right) E\{D_A\} \right]. \quad (A7)$$

Take the limit, $(\Delta y \rightarrow 0)$, and move $G(y)$ to the left-hand side of the equation. It is noted that the limiting values for F_i and $E\{D_A\}$ have already been inserted:

$$\frac{dG(y)}{dy} + \left(\frac{3}{y} \right) G(y) = \left[\frac{1}{(Ay)} \right] [-(x_2 y_1 - x_1 y_2) F_1 + (x_2 y_3 - x_3 y_2) F_2 + (x_3 y_4 - x_4 y_3) F_3 - (x_1 y_4 - x_4 y_1) F_4 + AE\{D_A\}]. \quad (A8)$$

In this equation all points, lines, and areas have their original (starting) values because $k = 1$ at the taken limit.

All terms on the right-hand side of Equation A8 can be written as functions of y , which can be used as a scaling variable during any dilation transformation. It is observed that these functions have the following proportional relationships to y under dilation: $x_i \propto y$, $y_i \propto y$, $F_i \propto y$, $E\{D_A\} \propto y$, and $A \propto y^2$. After factoring out and canceling y values the right-hand side of A8 is found to be a constant and will be designated C_0 . The differential equation is rewritten as

$$\frac{dG(y)}{dy} + \left(\frac{3}{y} \right) G(y) = C_0, \quad (A9)$$

where, before cancellation of y ,

yC_0

$$= \left\{ \frac{[-(x_2 y_1 - x_1 y_2) F_1 + (x_2 y_3 - x_3 y_2) F_2 + (x_3 y_4 - x_4 y_3) F_3 - (x_1 y_4 - x_4 y_1) F_4 + AE\{D_A\}]}{A} \right\}. \quad (A10)$$

Equation A9 is a linear differential equation of the first order for which the solution is found to be

$$G(y) = \frac{yC_0}{4}, \quad (A11)$$

where the value for yC_0 is given by A10. In obtaining this solution the constant of integration was found to be equal to 0 because when y (the scale variable) equals 0, G must also equal 0.

Essentially the same development is used to obtain the second moment, T , about the origin. Using formulas and notation provided in Greulich (2005) it is noted that S_i and $E\{D_A^2\}$ are both proportional to y^2 so that the differential equation becomes

$$\frac{dT(y)}{dy} + \left(\frac{3}{y} \right) T(y) = yC_1, \quad (A12)$$

where

$$y^2 C_1 = \frac{[-(x_2 y_1 - x_1 y_2) S_1 + (x_2 y_3 - x_3 y_2) S_2 + (x_3 y_4 - x_4 y_3) S_3 - (x_1 y_4 - x_4 y_1) S_4 + AE\{D_A^2\}]}{A}. \quad (A13)$$

The solution to this differential equation is given by

$$T(y) = \frac{y^2 C_1}{5}, \quad (A14)$$

with $y^2 C_1$ given by Equation A13.

With these results for the first two moments of the random distance between a line segment and a trapezoid, it is now possible to calculate the first two moments for the random distance between two trapezoids or between two random points within a single trapezoid. (It is left to the interested reader to extend these line segment-to-trapezoid results to the evaluation of transfer distances between rectifiable lines and polygonal regions.) The derivation procedure is fundamentally the same as was just applied for the calculation of G and T values.

With specific reference to Figure A2 in which a dilation of $1 + \Delta K$ has been applied, the following approximations to the incremental areas are obtained:

$$\Delta A_2 \approx (x_2 y_3) \left(\frac{\Delta y}{y} \right), \quad (A15a)$$

$$\Delta A_3 \approx (x_3 y_4 - x_4 y_3) \left(\frac{\Delta y}{y} \right), \quad (15b)$$

$$\Delta A_4 \approx (x_1 y_4) \left(\frac{\Delta y}{y} \right), \quad (15c)$$

$$\Delta B_6 \approx (x_6 y_7) \left(\frac{\Delta y}{y} \right), \quad (A15d)$$

$$\Delta B_7 \approx (x_7 y_8 - x_8 y_7) \left(\frac{\Delta y}{y} \right), \quad (A15e)$$

and

$$\Delta B_8 \approx (x_5 y_8) \left(\frac{\Delta y}{y} \right). \quad (A15f)$$

With specific reference to Figure A2 it is found that

$$\Delta A = \Delta A_2 + \Delta A_3 - \Delta A_4 = 2A \left(\frac{\Delta y}{y} \right), \quad (\text{A15g})$$

and

$$\Delta B = \Delta B_6 + \Delta B_7 - \Delta B_8 = 2B \left(\frac{\Delta y}{y} \right). \quad (\text{A15h})$$

Once again by applying Crofton's procedure the expected distance between a randomly located point within area $A + \Delta A$ and another located in area $B + \Delta B$ is found by conditioning on all possible locations in both cases. The indexing on G_i indicates the expected distance from the line forming trapezoid side i to the interior area of the other trapezoid:

$$\begin{aligned} H(y + \Delta y) = & \left[\frac{1}{(A + \Delta A)(B + \Delta B)} \right] \\ & \times [ABH(y) + A\Delta B_6 G_6 + A\Delta B_7 G_7 \\ & - A\Delta B_8 G_8 + \Delta A_2 B G_2 + \Delta A_3 B G_3 - \Delta A_4 B G_4]. \quad (\text{A16}) \end{aligned}$$

The resulting differential equation is

$$\frac{dH(y)}{dy} + \left(\frac{4}{y} \right) H(y) = \left[\frac{1}{(AB)y} \right] [yC_2], \quad (\text{A17})$$

where

$$\begin{aligned} yC_2 \equiv & [A(x_6 y_7)G_6 + A(x_7 y_8 - x_8 y_7)G_7 - A(x_5 y_8)G_8 \\ & + (x_2 y_3)BG_2 + (x_3 y_4 - x_4 y_3)BG_3 - (x_1 y_4)BG_4]. \quad (\text{A18}) \end{aligned}$$

After canceling out y on the right-hand side of Equation A17, the solution to this differential equation is found to be

$$H(y) = \frac{yC_2}{5AB}, \quad (\text{A19})$$

where yC_2 is given by Equation A18.

The second moment of the random distance from one trapezoid to the other is calculated as

$$U(y) = \frac{y^2 C_3}{6AB}, \quad (\text{A20})$$

where

$$\begin{aligned} y^2 C_3 \equiv & [A(x_6 y_7)T_6 + A(x_7 y_8 - x_8 y_7)T_7 \\ & - A(x_5 y_8)T_8 + (x_2 y_3)BT_2 + (x_3 y_4 - x_4 y_3)BT_3 \\ & - (x_1 y_4)BT_4]. \quad (\text{A21}) \end{aligned}$$

The first and second moments, H and U , for the random distance between two trapezoids have now been derived. These formulas, when used with their attendant computational procedures, provide the first two moments for any two trapezoids, whether disjoint, partially overlapping, or exactly overlapping.

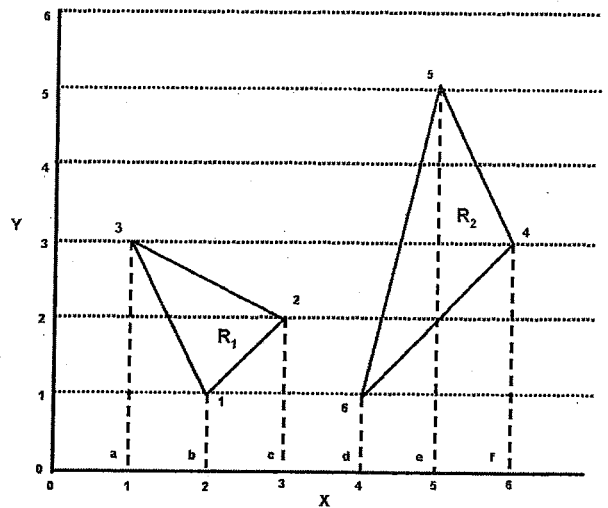


Figure B1. Two polygonal regions (both triangles) have their vertices uniquely numbered, each in a counterclockwise direction. The x -coordinates for these six vertices are lettered so that individual trapezoidal areas may be uniquely identified when referenced in the text.

Appendix B

The application of the trapezoid-to-trapezoid moment equations of Appendix A is most easily accomplished by using the coordinate area formula in the following manner. Each of two polygonal regions is delineated in the conventional manner with counterclockwise numbering of the vertices starting from an arbitrary vertex on each polygon. Figure B1 illustrates this delineation of two regions, which will be used as an example for the development that follows. (The reason for not numbering the vertices of R_2 starting with 1 will become clear in the development that follows, in which each of the six vertices must have a unique identifying number.)

Another way that the coordinate area formula may be written, using a counterclockwise orientation, is (Shih 1995)

$$A = \sum_{i=1}^n \left[\left(\frac{y_i + y_{i+1}}{2} \right) (x_i - x_{i+1}) \right]. \quad (\text{B1})$$

Here it is observed that each term in the expansion of this formula is the area of the trapezoid corresponding to a side of the region being traversed. For example, the first term in the area calculation of R_1 is $[(1/2)(y_1 + y_2)(x_1 - x_2)]$. It is noted that the sign of this particular area, trapezoid bc21, is negative because $x_2 > x_1$. The next term in the expansion of formula B1 corresponds to the area of trapezoid ac23 and is positive in sign. The final term, the area of trapezoid ab13, is negative. Adding these three terms leaves the area of region R_1 as a positive value. In this specific example

Table B1. Signed trapezoid areas calculated and summed for the six sides of the two triangles

	Trapezoid i	Area $_i$	Trapezoid j	Area $_j$
$i:$	1	-1.5	4	4.0
	2	5.0	5	3.0
	3	-2.0	6	-4.0
	SUM=	1.5	SUM=	3.0

Table B2. Signed cross products of the six trapezoid areas that are to be used as weights

(Area) _i (Area) _j	j			
	4	5	6	
1	-6.0	-4.5	6.0	
2	20.0	15.0	-20.0	
3	-8.0	-6.0	8.0	
SUM=	6.0	4.5	-6.0	4.5

$[-1.5] + [+5] + [-2] = 1.5$ square units of area in R_1 . These results for all three trapezoids of each region are given in Table B1.

Assume now that two random points are independently distributed. One of these points is distributed at random (uniformly) over the area ac23 (A_{ac23}), and the second point is distributed randomly over the area df456 (A_{df456}). It is required that the expected distance between these two points be calculated, given that the first point falls within R_1 and the second within R_2 .

The probability that the first point falls within R_1 is a function of the two areas, viz. $P\{123\} = (A_{123}/A_{ac23})$. Likewise for R_2 is obtained: $P\{456\} = (A_{456}/A_{df456})$. Now the probability that the first point falls within R_1 may also be written as the probability that it falls within area ac23, $P\{ac23\}$, minus the probability that it falls in either area ab13, $P\{ab13\}$, or area bc21, $P\{bc21\}$:

$$P\{123\} + [-P\{bc21\} + P\{ac23\} - P\{ab13\}]. \quad (B2a)$$

The same observations apply to R_2 , where, with attention to signs, the following is obtained:

$$P\{456\} = [P\{ef45\} + P\{de56\} - P\{df46\}]. \quad (B2b)$$

Substituting for the probabilities on the right-hand side of these two formulas,

$$P\{123\} = \left[-\frac{A_{bc21}}{A_{ac23}} + \frac{A_{ac23}}{A_{ac23}} - \frac{A_{ab13}}{A_{ac23}} \right], \quad (B3a)$$

and

$$P\{456\} = \left[\frac{A_{ef45}}{A_{df456}} + \frac{A_{de56}}{A_{df456}} - \frac{A_{df46}}{A_{df456}} \right]. \quad (B3b)$$

factoring out the denominator in each case and using the aforementioned coordinate area formula, these formulas may be conveniently written as

$$P\{123\} = \frac{1}{A_{ac23}} \sum_{i=1}^3 \left[\left(\frac{y_i + y_{i+1}}{2} \right) (x_i - x_{i+1}) \right], \quad (B4a)$$

Table B3. Expected flight distances between each of the mn ($3 \times 3 = 9$) trapezoids

H_{ij}	j		
	4	5	6
1	3.3959	2.5100	2.7530
2	3.8772	3.0214	3.3954
3	4.3786	3.5027	3.8746

where in this formula $(x_4, y_4) \equiv (x_1, y_1)$ and

$$P\{456\} = \frac{1}{A_{df456}} \sum_{j=4}^6 \left[\left(\frac{y_j + y_{j+1}}{2} \right) (x_j - x_{j+1}) \right], \quad (B4b)$$

where in this formula $(x_7, y_7) \equiv (x_4, y_4)$. It is observed in these equations that the appropriate signs are automatically applied to the calculated areas.

Because the two points are independently distributed, the joint probability that the first point falls in R_1 and the second in R_2 is the product of their individual probabilities, viz. $P\{123 \cap 456\} = P\{123\}P\{456\}$. Substituting B4a and B4b for $P\{123\}$ and $P\{456\}$, respectively, the following is obtained:

$$P\{123 \cap 456\} = \frac{1}{A_{ac23}A_{df456}} \sum_{i=1}^3 \sum_{j=4}^6 \left[\left[\left(\frac{y_i + y_{i+1}}{2} \right) (x_i - x_{i+1}) \right] \left[\left(\frac{y_j + y_{j+1}}{2} \right) (x_j - x_{j+1}) \right] \right]. \quad (B5)$$

The caution on i and j indexing previously mentioned for Equations B4a and B4b must also be observed here. The individual components in the numerator of this formula, $\{[Area_i][Area_j]\}$, are shown in Table B2. When divided by the quantity in the denominator, $A_{ac23}A_{df456}$, these individual terms give the probability that the random point falls within the corresponding trapezoid. These trapezoid probabilities are used for weighting the expected distances, H_{ij} , from trapezoid i to trapezoid j . The expected distances between trapezoids have been calculated as described in Appendix A, and their values for this example are given in Table B3. (Parenthetically it is noted that these numerical results provide an important intermediate computational check for future computer software programming.) In continuing with the current example of the nine pairings of trapezoids i and j , the weighted mean distance between R_1 and R_2 is found to be

$$H = \frac{\sum_{i=1}^3 \sum_{j=4}^6 \left\{ \left[\left(\frac{y_i + y_{i+1}}{2} \right) (x_i - x_{i+1}) \right] \left[\left(\frac{y_j + y_{j+1}}{2} \right) (x_j - x_{j+1}) \right] [H_{i,j}] \right\}}{\sum_{i=1}^3 \sum_{j=4}^6 \left\{ \left[\left(\frac{y_i + y_{i+1}}{2} \right) (x_i - x_{i+1}) \right] \left[\left(\frac{y_j + y_{j+1}}{2} \right) (x_j - x_{j+1}) \right] \right\}}. \quad (B6)$$

Cancellation of A_{ac23} and A_{df456} in numerator and denominator has already been done in this formula. The numerical value of the denominator in Equation B6 for the example at hand is shown as the final, right-hand sum in Table B2.

Shown here for two general triangles, this procedure may be applied to any two polygonal regions including those that are disjoint and (or) have excluded enclaves. It is also applicable to the analysis of random distances within a single polygonal region. It must be emphasized, if it is not already clear, that the polygonal regions do not have to be partitioned into triangles to apply this general procedure. For the specific example of this development, the results are an expected distance, H , of 3.2791, and an expected square of the distance, U , of 11.1667.

Appendix C

The results given in the body of this article have been calculated through the use of analytically derived formulas. These specific results have been independently checked by numerical methods to the number of digits shown in the article. A summary overview of the numerical method used to check these results is presented in this appendix.

The expected distance between a point (X, Y) randomly located within a triangular region of area A_1 , and a second point (S, T) randomly located within a different triangular region of area A_2 is given by

$$E\{D\} = \left[\frac{1}{A_1 A_2} \right] \iint_{A_1} \iint_{A_2} D(X, Y, S, T) dS dT dX dY, \quad (C1)$$

where

$$D(X, Y, S, T) = [(X - S)^2 + (Y - T)^2]^{1/2}. \quad (C2)$$

The numerical evaluation of this equation can be facilitated by a change of variables from (X, Y, S, T) to $(\tau_1, \tau_2, \eta_1, \eta_2)$ (Dahlquist and Björk 1974). The corners of each triangle are written using barycentric coordinates. Every point (X, Y) within this triangle can then be uniquely identified by the relationship

$$\begin{pmatrix} X \\ Y \end{pmatrix} = \begin{pmatrix} X_3 \\ Y_3 \end{pmatrix} + \tau_1 \begin{pmatrix} X_1 - X_3 \\ Y_1 - Y_3 \end{pmatrix} + \tau_2 \begin{pmatrix} X_2 - X_3 \\ Y_2 - Y_3 \end{pmatrix}, \quad (C3)$$

and the appropriate specification of τ_1 and τ_2 by this one-to-one linear mapping. For points falling within the triangle and on its boundary, the variables τ_1 and τ_2 assume values in the range $[0, 1]$ and the constraint $\tau_1 + \tau_2 \leq 1$ is imposed. Likewise for the second triangle where η_1 and η_2 assume values in the range $[0, 1]$ and the constraint $\eta_1 + \eta_2 \leq 1$ is imposed the relationship is

$$\begin{pmatrix} S \\ T \end{pmatrix} = \begin{pmatrix} S_3 \\ T_3 \end{pmatrix} + \eta_1 \begin{pmatrix} S_1 - S_3 \\ T_1 - T_3 \end{pmatrix} + \eta_2 \begin{pmatrix} S_2 - S_3 \\ T_2 - T_3 \end{pmatrix} \quad (C4)$$

and, finally then

$$\begin{aligned} \begin{pmatrix} X - S \\ Y - T \end{pmatrix} &= \begin{pmatrix} X_3 - S_3 \\ Y_3 - T_3 \end{pmatrix} + \tau_1 \begin{pmatrix} X_1 - X_3 \\ Y_1 - Y_3 \end{pmatrix} + \tau_2 \begin{pmatrix} X_2 - X_3 \\ Y_2 - Y_3 \end{pmatrix} \\ &\quad - \eta_1 \begin{pmatrix} S_1 - S_3 \\ T_1 - T_3 \end{pmatrix} - \eta_2 \begin{pmatrix} S_2 - S_3 \\ T_2 - T_3 \end{pmatrix}. \end{aligned} \quad (C5)$$

The determinant of the Jacobian for this transformation is

$2A_1 2A_2$ so that Equation C1 can be rewritten as

$$E\{D\} = 4 \int_0^1 \int_0^{1-\tau_1} \int_0^1 \int_0^{1-\eta_1} D(\tau_1, \tau_2, \eta_1, \eta_2) d\eta_2 d\eta_1 d\tau_2 d\tau_1, \quad (C6)$$

where substitution into the distance equation has been made using C5.

Any polygonal region can be completely divided into mutually exclusive triangular components. Typically there are many alternative ways that a polygonal region can be subdivided into triangles; for this analysis, however, no preferential way of subdividing the region was specified, and all are treated as being equally acceptable. The analysis of the random distance between two polygonal regions starts with the complete subdivision of each region into mutually exclusive triangular components. Each triangular component of one region, in turn, is numerically integrated with respect to every triangular component of the second region. All such triangle-to-triangle results are then combined by area (probability) weighting to provide the region-to-region results used in the verification process.

Developing a numerical integration approximation based on C6 starts with the formula

$$E\{D\} \approx 4 \sum_{i=1}^m \sum_{j=1}^n \sum_{k=1}^p \sum_{l=1}^q D(\tau_{1,i}, \tau_{2,j}, \eta_{1,k}, \eta_{2,l}) \Delta\eta_2 \Delta\eta_1 \Delta\tau_2 \Delta\tau_1, \quad (C7)$$

where $\tau_{1,i} = (1/m)(i - [1/2])$ and $\tau_{2,j} = (1/n)(j - [1/2])$ until $\tau_{2,j} \geq 1 - \tau_{1,i}$ with finite subdivisions $\Delta\tau_1 = 1/m$ and $\Delta\tau_2 = 1/n$. Likewise $\eta_{1,k} = (1/p)(k - [1/2])$ and $\eta_{2,l} = (1/q)(l - [1/2])$ until $\eta_{2,l} \geq 1 - \eta_{1,k}$ with finite subdivisions $\Delta\eta_1 = 1/p$ and $\Delta\eta_2 = 1/q$. This placement of the points (τ_1, τ_2) and (η_1, η_2) results in distance being measured from the center of the finite element in one triangle to the center of the finite element in the second triangle. Each of the finite elements within the original triangles is a parallelogram. An exception is noted for those elements falling along the extreme edge of each triangle, which are only half of a corresponding parallelogram element. This boundary effect becomes less significant as the number of subdivisions becomes larger. The actual number of subdivisions $m, n, p,$ and q is determined by the analyst's desired precision during the approximation process. Convergence is quite slow with this basic approach, and programming modifications that improve the convergence rate are possible. Such modifications are not presented here as they are peripheral to defining the basic numerical integration process and would unnecessarily complicate the presentation. A similar procedure was used to obtain a numerical estimate of the expected square of the random distance between two polygonal regions.

